HIGH SCHOOL EDITION
Journal of Student Research
Volume 12 Issue 3 (2023)

I131T Mutation's Effects on Van der Waals Forces and Solvation Energy in Congenital Hypothyroidism

Khoa Nguyen[1] and Oanh Vu[#]

[1]Lake Mary Preparatory School, USA
[#]Advisor

ABSTRACT

Garcia et al. (2017) unraveled the intricate mechanisms underlying the impact of the p.I131T mutation on the Thyrotropin Releasing Hormone Receptor (TRHR), a class A G-protein coupled receptor (GPCR). This mutation leads to Congenital Hypothyroidism in an 8-year-old patient with homozygosity and Hyperthyrotropinemia in heterozygous family members. The mutation substitutes a polar Thr for a non-polar Ile, disrupting the hydrophobic pocket within the TRHR-G-protein interface. While Molecular Dynamics (MD) simulations unveiled this interaction, the absence of experimental data on the activated TRH-TRHR-G protein complex hindered a comprehensive assessment. Addressing this gap, when Youwei Xu et al. (2022) recently presented the Cryo-EM structure of the activated complex, we employed Rosetta (Alford, et al., 2017) to optimize this structure and generated 100 starting structures; the five best ones were used as starting template structures to produce protein structures for both wild-type and mutant TRHR-TRH-G protein complexes. Our study not only validated Garcia et al.'s findings on reduced signal transduction but also pinpointed critical chemical interactions affected by the p.I131T mutation—specifically, Van der Waals forces and Solvation energy.

Introduction

In humans, especially children, the thyroid hormones (THs), with the two most major ones being T3 and T4, play an essential role in energy metabolism, growth, and neurodevelopment. Specifically, the thyroid hormone acts on neuronal differentiation, synapsis development, and myelination in the prenatal and newborn periods, regulating central nervous system development. As such, those with Congenital Hypothyroidism (CH), a disorder characterized by a thyroid hormone deficiency, are prone to irreversible neurological deficits (National Center for Biotechnology Information, n.d.). THs deficiency in fetal and neonatal periods results in cretinism, a disease characterized by mental retardation, deafness, and ataxia (Schroeder & Privalsky, 2014) with some cases of extremely low T4 levels even linked to psychiatric disorders like schizophrenia and autism (Uchida & Suzuki, 2021). A previous study even found correlation between CH and higher risk of congenital malformations (Rastogi & LaFranchi, 2010).

In patients without normal thyroid functions, thyroid hormones levels are controlled by a negative feedback loop: when low T3 and T4 levels occur, the hypothalamus secretes Thyrotropin Releasing Hormone (TRH) to activate the TRH receptor (TRHR), a G-protein–coupled receptor (GPCR) located at pituitary thyrotrophs, which then releases the G-protein alpha subunit to trigger a PKC pathway to release thyroid-stimulating hormone (TSH); these molecules stimulates the thyroid to produce thyroid hormones until levels in the bloodstream return to normal.

The mutation in the TRHR gene that replaces the isoleucine at position 131 into threonine (p.I131T) was discovered by a clinical study in 2017 by Garcia et al. This mutation caused moderate CH in homozygotes

and hyperthyrotropinemia in heterozygotes, with elevated TSH compensating for reduced T4. Garcia et al. (2017) studied a male patient who was not detected by a TSH-based neonatal screening program at birth, yet clinical evaluations when he was 8 suggested abnormal thyroid functions. Although he did not present symptoms of hypothyroidism, had normal stature and was only mildly overweight , all available TSH-T4 paired tests showed below average T4 levels while TSH levels were above average, signifying hypothyroidism. After four of his family members were discovered to have mildly elevated TSH levels with normal T4 levels, the researchers suspected that there was a genetic cause for the patient's hypothyroidism. By directly sequencing the coding exons of four candidate genes for central hypothyroidism (TRH, TRHR, TSHB, and IGSF1) for the patient's family, Garcia et al. concluded that the thyroidal pathologies observed can be fully attributed to the I131T mutation in the TRHR gene of the patient.

Garcia et al. (2017) assessed wild-type and I131T TRHR mutant in vitro through TRH binding affinity, and signal transduction assays. The authors reported that the TRHR mutant showed a three-fold decrease in ligand affinity. However, wild-type TRHR displayed over 10-fold higher AP1-luciferase activity upon TRH induction, highlighting the stronger impact of altered TRHR-Gq interface on cascade activation than lowered ligand affinity. They also performed molecular dynamics simulations on a "active-like" TRH-TRHR-Gq complex, which suggested that the mutation disrupted interactions between the receptor and Gq alpha sub unit's hydrophobic pocket. This observation from the MD simulations is consistent with their in vitro assay results.

Interestingly, five years after Garcia et al.'s study, in 2022, Youwei Xu et al. published the first active state Cryo-EM structure of the TRH-TRHR-Gq protein complex (Maradi et al.,2022). Since Garcia et al. only perform computational simulation on an "active-like" model of the TRHR in complex with Gq built with homology modeling (cite?). This approach towards computational simulation of the TRHR's I131T mutant analysis, however, is not as preferable as having experimental data on the structure of the actual protein complex. This prompts us to update and re-evaluate the molecular mechanism of the I131R mutant presented in Garcia et al., this time with an active state experimental starting structure and a more cost-effective protein modeling software that has never been used to study this mutation before: Rosetta (Alford et al., 2017). This software evaluates and optimizes protein structures by combining Monte-Carlo with simulated annealing to search for physically plausible molecular structures. Hence, Rosetta could be used to model the structure of the I131T TRHR mutant. Energy of non-covalent interactions, such as Van Der Waals forces and solvation energy, among residues can be broken down and further examined, allowing for a thorough analysis of the changes in binding energy caused by the substitution mutation I131T. The effects of the point mutation from Isoleucine to Threonine in TRHR on the interface between TRHR and the alpha subunit of the Gq protein were evaluated at the molecular level on multiple wild-type and mutated models of the protein complex.

Methods

Cryo-EM Structure Optimization and Parameterization of TRH

We generated a params file for the ligand using molfile_to_params.py script in Rosetta, which contains all the information on its geometry and chemistry that are compatible with Rosetta.

Utilizing the conformer generator application (Mendenhall et al., 2021) in the BioChemical Library (Brown et al., 2022), we generated a 3D conformer library for the ligand that allows for more flexibility in docking the TRH ligand into TRHR.

Since we are only looking to further optimize the Cryo-EM structure with Rosetta (Alford et al., 2017), we performed FastRelax on the whole protein structure with constraints placed on the coordinates of backbone heavy atoms. Using this protocol, we generated 100 models and used the best 5 in terms of Rosetta total score as starting templates for the next computational calculations.

Generating Wild-Type and I131T Mutant TRH-TRHR-G Protein Complexes Models Using Rosetta

With the 5 starting structures, we introduced the p.I131T mutation to TRHR by changing the residue type of the 131R (the residue id of the mutation position in the pdb file (PDB id: 7WKD)) from Isoleucine to Threonine using the MutateResidue mover in Rosetta (Alford et al., 2017). Then, we ran FastRelax on the 5 temps without any coordinate constraints so as to see how the mutant affects the backbone conformations alongside the side-chain conformations (documented as mutate.full_Relax in supplementary information). We generated 50 structures for each template.

We also performed the same protocol on the five template structures without introducing the mutation. This is so that all the models, wild-type or native, went through the same number of rounds of FastRelax, which ensures any differences in energy between the wild-type and native structures can be attributed to the mutation and not an algorithmic bias towards the models for the wild-type. We generated 50 structures for each template.

Rosetta Score Analysis: Comparison Between the Wild-Type and I131T Mutant

To evaluate the mutant's effects on the TRHR-Gqa binding interface and the protein structure in general, for all five starting template structures, we compared the protein structures of wild-type and I131T mutated in terms of the mean values of Rosetta total model scores, separation energy score and change in solvent accessible area at the TRHR-Gqa subunit interface. The difference in separation energy at the TRHR-TRH ligand site between the wild-type and mutated protein models was also evaluated.

Using the residue energy breakdown application (Leman, et al., 2020) in Rosetta (Alford, et al., 2017), we collected data on the energy of various kinds of chemical interactions between the 131R residue and the residues of the alpha subunit of the G-protein to study the change in interface score due to the mutation at the molecular level.

We then utilized Python and the Pandas, NumPy and SciPy packages in performing the t-test so as to compare the data on total model scores, separation energy at the interface of interest, and individual scoring terms for each residue pair between the mutated and wild-type models for each of the 5 templates.

Results

In Rosetta, the Rosetta energy of a structure is calculated as the linear sum of weighted scoring terms of various non-covalent interactions such as Hydrogen bonds, Van Der Waals, and solvation energy, etc. In this study, REF2015, the most updated standard scoring function of Rosetta, was used to score WT and I131T TRHR mutant models..

Rosetta's -FastRelax application performs multiple iterations of sidechain repacking and minimization to refine the energy of a structure in the Rosetta force-field.. by making small alterations to the backbone and side chain torsion angles, with each "move" accepted or denied based on the Metropolis–Hastings algorithm so as to search for the structure conformation at a local minimum of the energy function. It searches for the local minima in the conformational space around the starting structure. Hence, this application is ideal for modeling minor changes on a previously idealized experimental structure of THRR.

Mutating Residue Reduced the Total Score and Interaction Energy Score Between TRHR and Alpha Subunit

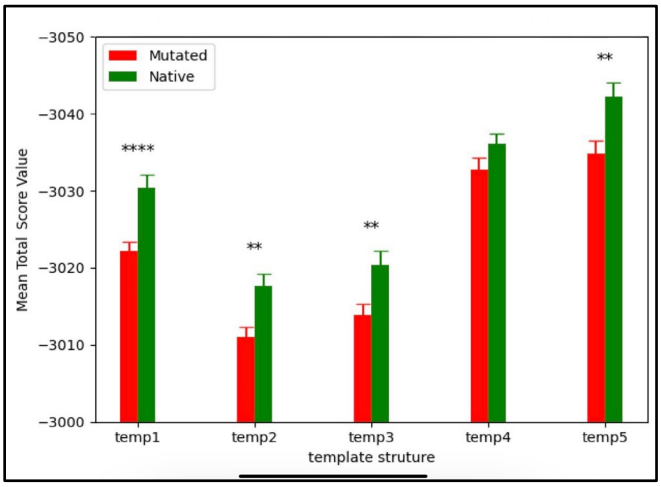

Figure 1. The difference in the mean Rosetta Total Score of the models of native and mutated TRH-TRHR-G protein complex generated from the 5 templates. n=50. Error bars represent 1 S.E. **p<0.01. ****p<0.00001. Table S1 in the Supplemental Information contains information, for all five templates, on the difference in total score between the mutant and wild-type, the p-value to six decimal places, and the standard error for the mutant and wild-type.

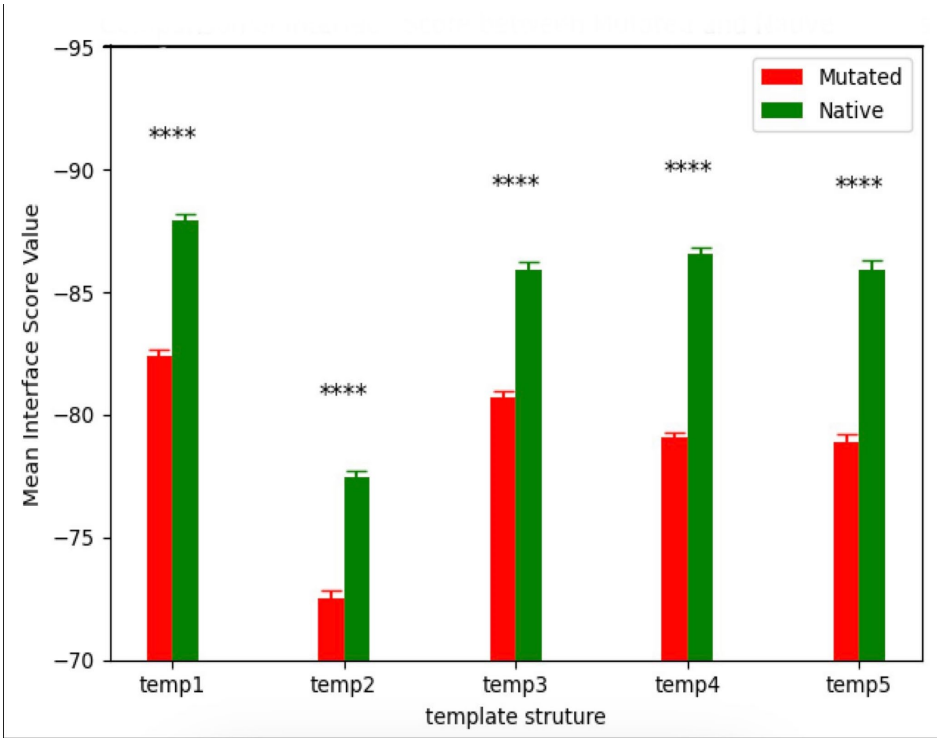

Figure 2. The difference in the mean Interface Score (or separation energy) of the models of native and mutated TRH-TRHR-G protein complex generated from the 5 templates. n=50. Error bars represent 1 S.E.

****p<0.0001. Table S2 in the Supplemental Information contains information, for all five templates, on the difference in separation energy between the mutant and wild-type, the p-value to six decimal places, and the standard error for the mutant and wild-type.

In four out of the five starting templates, the mean Rosetta total score for the wild-type models generated by FastRelax is consistently lower than that of mutated models, with p-values between the total scores of the two groups lower than 0.01 for all of the templates (Figure 1). This signifies the lower stability of the mutated structure compared to the wild-type, which demonstrates the destabilizing effect of the mutation p.I131T on the TRH-TRHR-G protein complex as a whole. The same can be said for the separation energy at the TRHR - alpha subunit of the Gq protein, as the mean interface score for the wild-type is are lower than that of the mutant protein structures and p-values lower 0.0001 across all five templates (Figure 2). The drop in separation energy denotes the interference the I131T mutation causes on the binding energy between TRHR and the alpha subunit.

Per-Residue Score Analysis Suggested that the Effects of I131T Were Due to Changes in Interactions Between the Mutated Residue and the Nearby Hydrophobic Pocket.

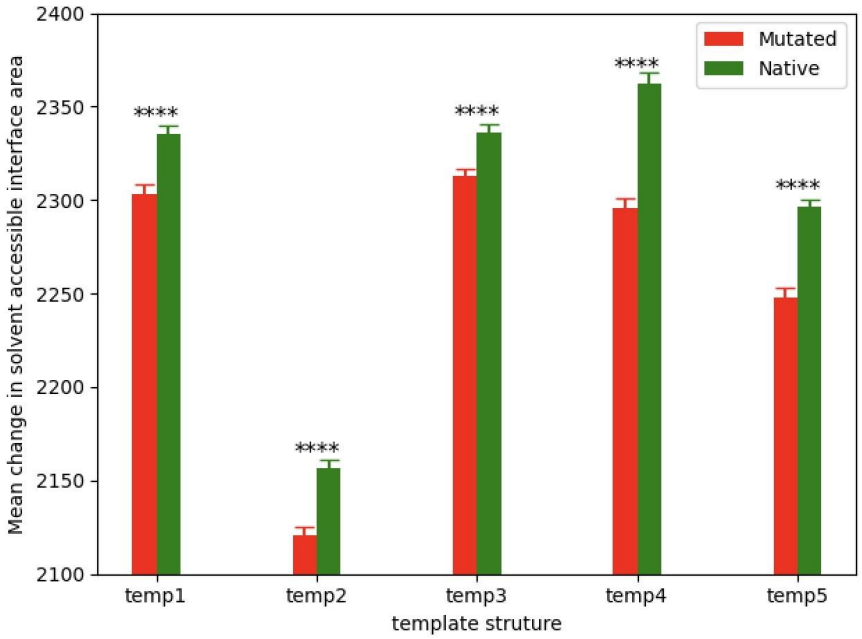

Figure 3. The difference in the mean Solvent Accessible Area at the TRHR-Gq interface of mutant and wild-type models generated from the five starting templates. n = 50. Error bars represent 1 S.E. ****p<0.0001. Table S3 in the Supplemental Information contains information, for all five templates, on the difference in mean change in solvent accessible area between the mutant and wild-type, the p-values to six decimal places, and the standard error for the mutant and wild-type.

Residue id	residue type	fa_atr	fa_rep	fa_sol	total
34A	Leu	0.714	0.056	0.642	1.297
194A	Val	0.539	0.255	0.929	1.155
196A	Phe	0.113		0.080	0.191
343A	Phe	0.796	0.020	0.614	1.411
346A	Cys	0.199		0.018	0.207
347A	Lys	1.026	0.010	0.042	0.956
350A	Ile	0.628	0.181	0.238	0.637
354A	Asn	0.002		0.005	0.006

Figure 4. The difference between the mean values of each Rosetta scoring term for chemical interactions between the 131R residue and residues of the Gq subunit alpha. Residue ids are those used for the residues in the PDB file 7WKD. Red indicates that the value for the interaction between mutant residue and the residue of that row is higher than that of the wild-type residue, which means it is less favorable, while green indicates the opposite. Cyan-colored residues are hydrophobic. Fa_atr, fa_rep, fa_sol and total represent attractive Van der Waals energy, repulsive Van der Waals energy, solvation energy and total residue pair Rosetta energy score, respectively.

The significant drop in Rosetta total structure energy score and separation energy in mutant models (Figures 1, 2) elicit the need to examine the residue-level energy changes that occur with the introduction of the I131T mutation to the protein structure. We used the residue energy breakdown application (Leman, et al., 2020) in Rosetta (Alford, et al., 2017) to study in depth the chemical interactions between the 131R residue and residues of the alpha subunit; the application gives data not only physical energy and knowledge-based scoring terms but also gives a total energy score for each residue pair. Although there are various scoring terms in the Rosetta scoring function, we only included the differences in mean values of comparisons between wild-type and mutated residue with p-values smaller than 0.05 and ignored the ones without statistical significance - identified by conducting the t-test between the values of each scoring term for each residue pair for the wild-type and mutant models (Figure 4).

Specifically, we found a statistically significant, although modest, increase in the energy of attractive Van Der Waals interactions (fa_atr) and Solvation energy (fa_sol), and a mild decrease in that of repulsive Van Der Waals interactions, between the 131R residue and the residues of the alpha subunit at the coupling interface of all of the mutant models (Figure 4), suggesting less stable interactions compared to the wild-type structures. All the other types of residue-level chemical interactions that ref2015 calculates, such as coulombic electrostatic potential (fa_elec) or hydrogen bonds, did not show any significant changes ($p>0.05$). Thus, these results suggested that the substitution of Ile for Thr leads to a significant increase in the attractive Van Der Waals interactions and Solvation energy between the residues of the alpha subunit and the 131R residue, which negates the slight decrease in repulsive Van Der Waals energy, interfering with the coupling of TRHR and G-protein. With a deeper understanding of the that the kinds of chemical interactions that the mutation affects are Van Der Waals interactions and Solvation energy, we then can provide more detailed analysis and reasoning on the mechanism through which the point mutation from Isoleucine to Threonine affected these interactions with the residues of the alpha subunit at the interface by examining the molecular and functional differences between Isoleucine and Threonine.

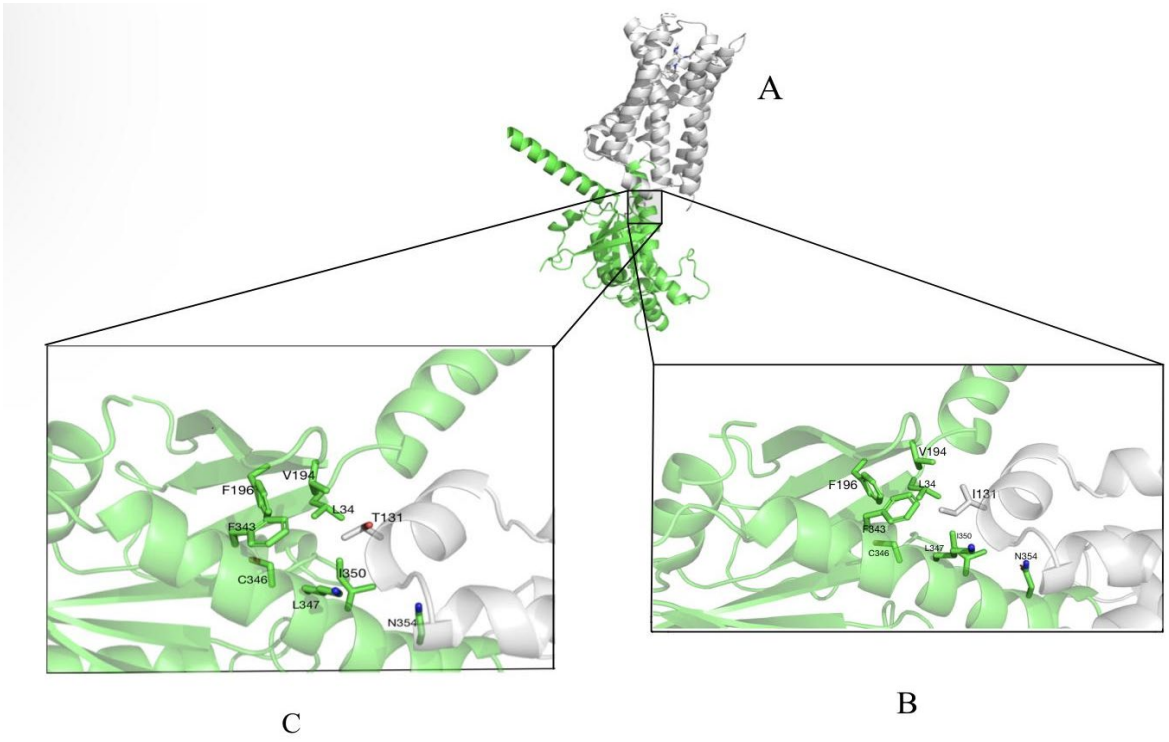

Figure 5. Overall view of the TRH -TRHR-G protein subunit alpha complex (A), with TRHR colored grey and the alpha subunit colored green, and zoomed in illustration of the wild-type residue I131 and the residues of the alpha subunit that it interacts with and collectively create a hydrophobic pocket (B), as well as one of the mutant T131 interacting with those residues (C)

As seven of the eight residues of the alpha subunit at the interface are hydrophobic and the wild-type residue Isoleucine has a nonpolar side chain (Kyte & Doolittle, 1982), the interaction energy between I131 and this pocket would be mainly driven by hydrophobic interactions (Figure 5B). Additionally, based on the calculations performed by Rosetta, the attractive Van Der Waals interactions play an important role in strengthening this effect between these residues, which further stabilizes the TRHR-alpha subunit interface. However, Threonine, with a volume of 116.1 cubic Å (Zamyatnin, 1972), is not only polar, which deranges the hydrophobic interaction at the TRHR-Gq interface, but also has a much smaller volume than Isoleucine, which has a volume of 166.7 cubic Å ((Zamyatnin, 1972). This means it has a smaller electron cloud than Ile does, and thus has weaker Van Der Waals interactions with the residues of the alpha subunit.

We actually have further computational evidence for I131T's intruding the hydrophobic pocket: the higher solvation energy. The increase in solvation energy in mutant model structures (Figure 4) could mean that the mutated residue has more favorable interactions with the water molecules in the solvent than the wild-type does and interferes with the hydrophobic pocket, which is consistent with the difference in hydrophobicity between Threonine, a polar amino acid, and Isoleucine, a non-polar amino acid. Additionally, we found that mutant models have consistently lower changes in solvent accessible areas than in wild-type models (Figure 3). This may suggest that the residues in the hydrophobic pocket are more packed with the wild-type I131 residue than with the T131 mutated residue.

Discussion

Although Garcia et al. showed the disruptive nature of the p.I131T mutation by performing signal transduction assay using an AP1-luciferase reporter and recording a ten-fold decrease in the activity of this reporter in cells with the mutated TRHR, their experiment did not elucidate on the fundamental molecular changes at the TRHR-Gq binding interface that the mutation caused; they attempted to study these alterations with MD simulations on a starting model structure of the active TRH-TRHR-G protein complex built with templates from other protein structures without having any experimental data on the actual conformation of the desired complex. Despite their best efforts to select templates with enough similarity to the amino acid chains of the protein complex in question, they could only identify four residues of the G-protein that interacted with the 131R residue, and reported no chemical energy calculations on these residues. Since all of the four residue that they identified were hydrophobic, as is the wild-type residue Isoleucine, and the mutant residue, Threonine, has a polar sidechain, Garcia et al. asserted that this occurrence of a polar side chain disrupted TRHR-Gq coupling. However, using a starting structure experimentally supported with Cryo-EM, we identified the residues of interest of the alpha subunit at the TRHR-Gq interface, of which there are eight, but the software also determined the energy levels of various chemical interactions between these residues and the 131R residue, allowing for a more thorough analysis of the fundamental molecular changes that the substitution mutation caused on the TRHR-Gq interface, rather than just a proposition, like in Garcia et al.'s research.

Unlike any other recorded mutations in the gene coding for TRHR, such as R17X (Bonomi et al., 2019), S115-T117del+A118T (Collu et al., 1997), and P81R (Koulouri et al., 2016), in which either the transmembrane domains or the ligand binding pocket is affected, the I131T mutation impedes TRHR's coupling with the alpha subunit of the G-protein, making it the first of its kind among the TRHR mutations, as well as the most we have the least amount of understanding on. In our research, despite having gained more knowledge on how this mutation interferes with the TRHR-Gq interface, especially at the molecular level, the process through which it affects TRH binding remains unknown to us.

Although Garcia et al. performed a ligand-affinity assay and recorded a three-fold decrease in TRH affinity in the mutant TRHR, they did not provide an explanation with regard to the mutation, since its position in the protein structure is too far away from the ligand binding site; they proposed that the suboptimal coupling to the G-protein could affect ligand binding. Taking into account that the G-protein is known to allosterically couple with the binding site in GPCRs (DeVree et al., 2016), there is merit to their claim. However, Rosetta neither produced results that bear any resemblance to the ones demonstrated in the experiment nor elucidate on the G-protein allosteric coupling hypothesis, as there is no statically significant change between the separation energy at the ligand-binding site of wild-type and mutant models across all five starting templates (data included in Supplemental Information, table S4 and figure SG1). This result does not cast doubt on the accuracy of the ligand affinity assay, but rather calls into question the capabilities of Rosetta in general, and more specifically of FastRelax, in modeling more subtle influences of a minute change in residue type on the confirmation of a residue distant from the mutation site. Future studies evaluating the p.I131T mutation's effects on the ligand binding site that accounts for more subtle yet potentially influential variables, such as quantum level changes. One such method is molecular dynamics simulation with an explicit membrane system (Mackerell et al.,1998), which was used in the discovery of a new allosteric binding site in GPCRs (Dror et al., 2011). Furthermore, another potential limitation of this study is the usage of REF2015, as optimized a scoring function for soluble proteins, might not be ideal for scoring membrane protein such as TRHR. However, since we only modeled a single point mutation, which is located at intracellular loop 2 and is at the interface with the alpha subunit, it is still acceptable for scoring the interface in this instance.

The p.I131T mutation is special in its affecting both GPCR-G protein coupling and ligand binding despite being too distantly located from the ligand binding site to play a role in stabilizing the ligand pocket. Schöneberg and Liebscher (2021) characterized the mechanisms through which GPCR mutations affect GPRC

activity and only found mutations that either affect GPCR-G protein coupling or ligand affinity. Thus, it would not be surprising if similar mutations to I131T exist but have not been discovered, and large-scale clinical studies could be done to search for these mutations. Possible flags for them could be a significant change in hydrophobicity or volume of the amino acid type, as well as the position of the mutant residue being close or at the G-protein coupling interface, especially if there is a hydrophobic or hydrophilic pocket.

Conclusion

By analyzing the new active-state TRHR-G protein complex structure, we not only confirmed the change in residue polarity that I131T mutation brought about at the hydrophobic pocket at the TRHR- alpha subunit interface that Garcia et al. discovered, but also found that the mutation increases the total energy of the protein complex, as well as the separation energy at the interface. We also identified the main chemical interactions that this mutation affected at this interface are Van der Waals forces, along with the hydrophobic effect and solvation energy. This study examined the molecular mechanism of action of an understudied I131T mutant on TRHR that reduced its activation, causing mild hypothyroidism.

Acknowledgment

I would like to thank Oanh Vu from the bottom of my heart for her passion (and patience) in guiding me through the intricate usage of Rosetta as well as more advanced concepts in biochemistry. I most likely would not have even completed the project if it were not for her encouragement and mentorship.
Thank you Mr. Mario Martinez for teaching me how to code and deal with data.
Thank you ChatGPT for its assistance in debugging the Python codes used in data analysis.

References

Abelian, A., Dybek, M., Wallach, J., Gaye, B., & Adejare, A. (2021). Chapter 6 - Pharmaceutical Chemistry. In A. Adejare (Ed.), *Remington (Twenty-third Edition)* (pp. 105-128). Academic Press. ISBN 9780128200070. https://doi.org/10.1016/B978-0-12-820007-0.00006-4

Alford, R. F., Leaver-Fay, A., Jeliazkov, J. R., O'Meara, M. J., DiMaio, F. P., Park, H., Shapovalov, M. V., Renfrew, P. D., Mulligan, V. K., Kappel, K., Labonte, J. W., Pacella, M. S., Bonneau, R., Bradley, P., Dunbrack Jr., R. L., Das, R., Baker, D., Kuhlman, B., Kortemme, T., & Gray, J. J. (2017). The Rosetta All-Atom Energy Function for Macromolecular Modeling and Design. *Journal of Chemical Theory and Computation, 13*(6), 3031-3048. http://doi.org/10.1021/acs.jctc.7b00125

Bonomi, M., Busnelli, M., Beck-Peccoz, P., Costanzo, D., Antonica, F., Dolci, C., Pilotta, A., Buzi, F., & Persani, L. (2009). A family with complete resistance to thyrotropin-releasing hormone. *The New England journal of medicine*, *360*(7), 731–734. https://doi.org/10.1056/NEJMc0808557

Brown, B. P., Vu, O., Geanes, A. R., Kothiwale, S., Butkiewicz, M., Lowe, E. W., Mueller, R., Pape, R., Mendenhall, J., & Meiler, J. (2022). Introduction to the BioChemical Library (BCL): An Application-Based Open-Source Toolkit for Integrated Cheminformatics and Machine Learning in Computer-Aided Drug Discovery. *Frontiers in Pharmacology, 13*, 833099. https://doi.org/10.3389/fphar.2022.833099

Collu, R., Tang, J., Castagné, J., Lagacé, G., Masson, N., Huot, C., Deal, C., Delvin, E., Faccenda, E., Eidne, K. A., & Van Vliet, G. (1997). A novel mechanism for isolated central hypothyroidism: inactivating mutations in the thyrotropin-releasing hormone receptor gene. *The Journal of clinical endocrinology and metabolism*, *82*(5), 1561–1565. https://doi.org/10.1210/jcem.82.5.3918

DeVree, B. T., Mahoney, J. P., Vélez-Ruiz, G. A., Rasmussen, S. G., Kuszak, A. J., Edwald, E., Fung, J. J., Manglik, A., Masureel, M., Du, Y., Matt, R. A., Pardon, E., Steyaert, J., Kobilka, B. K., & Sunahara, R. K. (2016). Allosteric coupling from G protein to the agonist-binding pocket in GPCRs. *Nature, 535*(7610), 182–186. https://doi.org/10.1038/nature18324

Dror, R. O., Pan, A. C., Arlow, D. H., Borhani, D. W., Maragakis, P., Shan, Y., Xu, H., & Shaw, D. E. (2011). Pathway and mechanism of drug binding to G-protein-coupled receptors. *Proceedings of the National Academy of Sciences of the United States of America*, *108*(32), 13118–13123. https://doi.org/10.1073/pnas.1104614108

Fleishman, S. J., Leaver-Fay, A., Corn, J. E., Strauch, E. M., Khare, S. D., Koga, N., Ashworth, J., Murphy, P., Richter, F., Lemmon, G., Meiler, J., & Baker, D. (2011). RosettaScripts: A scripting language interface to the Rosetta macromolecular modeling suite. PLoS ONE, 6(6), e20161. https://doi.org/10.1371/journal.pone.0020161

García, M., González de Buitrago, J., Jiménez-Rosés, M., Pardo, L., Hinkle, P. M., & Moreno, J. C. (2017). Central Hypothyroidism Due to a TRHR Mutation Causing Impaired Ligand Affinity and Transactivation of Gq. *The Journal of Clinical Endocrinology and Metabolism, 102*(7), 2433–2442. https://doi.org/10.1210/jc.2016-3977

Jumper, J et al. (2021). Highly accurate protein structure prediction with *AlphaFold*. *Nature, 596*, 583–589. https://doi.org/10.1038/s41586-021-03819-2

Koulouri, O., Nicholas, A. K., Schoenmakers, E., Mokrosinski, J., Lane, F., Cole, T., Kirk, J., Farooqi, I. S., Chatterjee, V. K., Gurnell, M., & Schoenmakers, N. (2016). A Novel Thyrotropin-Releasing Hormone Receptor Missense Mutation (P81R) in Central Congenital Hypothyroidism. *The Journal of clinical endocrinology and metabolism*, *101*(3), 847–851. https://doi.org/10.1210/jc.2015-3916

Kyte, J., & Doolittle, R. F. (1982). A simple method for displaying the hydropathic character of a protein. *Journal of Molecular Biology, 157*(1), 105–132. https://doi.org/10.1016/0022-2836(82)90515-0

Leman, J. K., Weitzner, B. D., Lewis, S. M., et al. (2020). Macromolecular modeling and design in Rosetta: recent methods and frameworks. *Nature Methods, 17*(7), 665–680. https://doi.org/10.1038/s41592-020-0848-2

MacKerell, A. D., Bashford, D., Bellott, M., Dunbrack, R. L., Evanseck, J. D., Field, M. J., Fischer, S., Gao, J., Guo, H., Ha, S., Joseph-McCarthy, D., Kuchnir, L., Kuczera, K., Lau, F. T., Mattos, C., Michnick, S., Ngo, T., Nguyen, D. T., Prodhom, B., Reiher, W. E., … Karplus, M. (1998). All-atom empirical potential for molecular modeling and dynamics studies of proteins. *The journal of physical chemistry. B*, *102*(18), 3586–3616. https://doi.org/10.1021/jp973084f

Mendenhall, J., Brown, B. P., Kothiwale, S., & Meiler, J. (2021). BCL::Conf: Improved Open-Source Knowledge-Based Conformation Sampling Using the Crystallography Open Database. *Journal of Chemical Information and Modeling, 61*(1), 189-201. https://pubs.acs.org/doi/10.1021/acs.jcim.0c01140

National Center for Biotechnology Information. (n.d.). Congenital Hypothyroidism. In *GeneReviews*®. Retrieved August 17, 2021, from https://www.ncbi.nlm.nih.gov/books/NBK558913/

Rastogi, M. V., & LaFranchi, S. H. (2010). Congenital hypothyroidism. *Orphanet Journal of Rare Diseases, 5*, 17. https://doi.org/10.1186/1750-1172-5-17

Schöneberg, T., & Liebscher, I. (2021). Mutations in G Protein-Coupled Receptors: Mechanisms, Pathophysiology and Potential Therapeutic Approaches. Pharmacological reviews, 73(1), 89–119. https://doi.org/10.1124/pharmrev.120.000011

Schroeder, A. C., & Privalsky, M. L. (2014). Thyroid hormones, T3 and T4, in the brain. *Frontiers in Endocrinology, 5*. https://doi.org/10.3389/fendo.2014.00040

Stoupa, A., Kariyawasam, D., Polak, M., & Carré, A. (2022). Genetics of congenital hypothyroidism: Modern concepts. *Pediatric Investigation, 6*, 123–134. https://doi.org/10.1002/ped4.12324

Uchida, K., & Suzuki, M. (2021). Congenital Hypothyroidism and Brain Development: Association With Other Psychiatric Disorders. *Frontiers in Neuroscience, 15*, 772382. https://doi.org/10.3389/fnins.2021.772382

Varadi, M., et al. (2022). AlphaFold Protein Structure Database: massively expanding the structural coverage of protein-sequence space with high-accuracy models. Nucleic Acids Research. https://doi.org/10.1093/nar/gkab1061

Xu, Y., Cai, H., You, C., He, X., Yuan, Q., Jiang, H., Cheng, X., Jiang, Y., & Xu, H. E. (2022). Structural insights into ligand binding and activation of the human thyrotropin-releasing hormone receptor. *Cell Research, 32*(9), 855–857. https://doi.org/10.1038/s41422-022-00641-x

Zamyatnin, A. A. (1972). Protein volume in solution. Progress in Biophysics and Molecular Biology, 24, 107-123. https://doi.org/10.1016/0079-6107(72)90005-3